NASA TECHNICAL NOTE

NASA TN D-5609

NASA TN D-5609

SIMPLIFIED ANALYSIS OF NUCLEAR FUEL PIN SWELLING

by Armin F. Lietzke

Lewis Research Center

Cleveland, Ohio

NATIONAL AERONAUTICS AND SPACE ADMINISTRATION • WASHINGTON, D. C. • JANUARY 1970

1. Report No. NASA TN D-5609	2. Government Accession No.	3. Recipient's Catalog No.
4. Title and Subtitle SIMPLIFIED ANALYSIS OF NUCLEAR FUEL PIN SWELLING		5. Report Date January 1970 6. Performing Organization Code
7. Author(s) Armin F. Lietzke		8. Performing Organization Report No. E-5145
9. Performing Organization Name and Address Lewis Research Center National Aeronautics and Space Administration Cleveland, Ohio 44135		10. Work Unit No. 120-27 11. Contract or Grant No. 13. Type of Report and Period Covered Technical Note
12. Sponsoring Agency Name and Address National Aeronautics and Space Administration Washington, D.C. 20546		14. Sponsoring Agency Code

15. Supplementary Notes

16. Abstract

The effect of fuel swelling on strains in the cladding of cylindrical fuel pins is analyzed. Simplifying assumptions are made to permit solutions for strain rates in terms of dimensionless parameters. The results of the analysis are presented in the form of equations and graphs which illustrate the volumetric swelling of the fuel and the strain rate of the fuel pin clad.

17. Key Words *(Suggested by Author(s))* Nuclear fuel Fuel element Fuel swelling	18. Distribution Statement Unclassified - unlimited		
19. Security Classif. (of this report) Unclassified	20. Security Classif. (of this page) Unclassified	21. No. of Pages 42	22. Price* $3.00

*For sale by the Clearinghouse for Federal Scientific and Technical Information
Springfield, Virginia 22151

SIMPLIFIED ANALYSIS OF NUCLEAR FUEL PIN SWELLING

by Armin F. Lietzke

Lewis Research Center

SUMMARY

The effect of fuel swelling on strains in the cladding of cylindrical fuel elements is analyzed. Simplifying assumptions are made to permit solutions for strain rates in terms of dimensionless parameters. The most significant assumptions included in the analysis are (1) the fission gases appear as bubbles dispersed throughout the fuel, (2) the bubble gas pressure is in equilibrium with the creep strength of the fuel, (3) uniform temperature exists in the fuel and in the clad, and (4) no axial force is transmitted between the fuel and the clad.

The results of the analysis are presented in the form of equations and graphs of dimensionless parameters which illustrate the volumetric swelling of the fuel and the strain rate of the fuel pin clad. A parameter is defined in terms of operating conditions, the value of which determines the strain rate of the clad relative to the volumetric swelling rate of the fuel.

Although the assumptions used to simplify the analysis restrict its application to special cases, the results show the relative importance of operating conditions and material creep properties for these cases and give some insight as to their importance for other cases. The assumptions involved make the analysis most suited to long operating lifetimes with low burnup rates, such as may be anticipated for space power reactor systems.

INTRODUCTION

Fuel elements of nuclear reactors are subject to internal stresses which may lead to large dimensional changes or gross failure. Of particular significance for long life, high power density reactors are those stresses resulting from a high concentration of fission products. Fission products cause the fuel to swell if retained in the fuel or, if released from the fuel, the gaseous products exert pressure on the clad material. In either case, some means must be provided to accommodate the fission products, other-

wise an intolerable stress will be produced in the clad.

The fuel element geometry frequently considered for severe operating conditions is a cylindrical fuel pin incorporating a void space, as illustrated in figure 1. The cylindrical clad forms an efficient pressure container, and the void space accommodates any fission gases released from the fuel and some degree of fuel swelling.

Several computer programs have been written to calculate stresses and strains in cylindrical fuel pins (e.g., ref. 1). Computer programs which take into account all aspects of the design problem, including heat transfer, thermal stress, and property variations as well as fission product swelling, are necessarily very complex. Design calculations utilizing such computer programs may require extensive iteration to arrive at a satisfactory solution and might best be utilized to check final designs.

The purpose of this report is to investigate only those stresses and strains caused by fuel swelling and through this simplification to express the calculated strains in terms of parameters that can more conveniently be used for design purposes. The swelling problem treated herein is the case where all fission products, both solid and gaseous, are contained within the fuel and contribute to fuel swelling. The analysis neglects elastic strains and first-stage creep. The analysis involves (1) the treatment of fuel swelling, and (2) the interaction of fuel and clad as the clad restrains the fuel from swelling radially outward.

Because fuel swelling is not fully understood, a calculational model must be hypothesized to explain the mechanism of the swelling process. Several models have been proposed. A model was proposed by Wyatt (ref. 2) to calculate swelling in uranium metal. This model assumes the gaseous fission products to accumulate at nucleation sites to form bubbles dispersed throughout the fuel material. The gas pressure in these bubbles stresses the fuel material, which strains in accordance with its creep properties. Essentially the same model was later used by Foreman (ref. 3) to calculate swelling rates in uranium. Foreman, however, used a more rigorous treatment of the stress distribution in the fuel. The methods of reference 3 are followed in the present work to calculate the volumetric swelling of the fuel.

A model for fuel swelling was also proposed by Barnes (ref. 4), which assumes the gas pressure forces to be in equilibrium with the forces of surface tension. The creep strength of the material was neglected. The model of reference 3 is preferred for the work herein for two reasons. First, high temperature applications will probably employ refractory fuel compounds having high creep strength. Secondly, although surface energy effects are important initially, long operating times at high temperature will probably result in bubbles large enough that surface tension effects may be neglected during most of the operating time.

The interaction of fuel and clad is analyzed by the use of multiaxial creep equations applied to thick-walled cylinders. The assumption is made when applying the boundary conditions that no axial force is transmitted between fuel and clad.

The analysis results in a set of equations expressing the strains in terms of creep properties, operating conditions, and geometric dimensions. Graphs of some of the equations are presented to aid in computations. A numerical example is given to illustrate the use of the figures and equations.

The equations to perform the numerical integrations included in this work were programmed by J. L. Thompson.

ANALYSIS

The methods used to calculate stresses and strains in a cylindrical fuel pin are as follows: Fuel volumetric swelling rates were calculated according to the model proposed by Wyatt (ref. 2) and modified by Foreman (ref. 3). These volumetric swelling rates are assumed to be independent of clad restraint, that is, clad restraint affects only the distribution of fuel strain in the radial, tangential, and axial directions. Using these volumetric swelling rates, the fuel and clad were then analyzed as radially loaded thick-walled cylinders having a common pressure at their interface; the fuel being radially loaded on its outside surface and the clad being radially loaded on its inside surface.

Multiaxial stresses appear in the fuel swelling model and in the fuel and clad cylinders as a result of their mutual interaction. The analytical treatment of steady-state creep under multiaxial stress appears in the prior literature (e.g., ref. 5). The equations based on this prior treatment are given in appendix B. All symbols are defined in appendix A.

Fuel Swelling

The analysis of fuel swelling caused by fission gas containment in the fuel follows that given in reference 3. The calculational model assumes gaseous fission products to accumulate at nucleation sites to form bubbles dispersed throughout the fuel. The fuel material is divided into polyhedral cells, each of which contains a gas bubble at the center. Each cell is approximated by a sphere of equal volume. The fuel swelling problem for gaseous fission products is thereby reduced to a determination of the creep of an internally pressurized thick-walled sphere. This latter case is also treated in reference 5.

The model neglects surface tension and assumes the fission gas pressure to be in equilibrium with the creep resistance of the fuel material. The only justification for this assumption other than to simplify the analysis would be to show experimentally that the fission gas bubbles are indeed large enough to make surface energy effects negligibly small. Until such evidence exists for any fuel in question, it may be argued that while surface energy effects are important initially (when the bubbles are small), the bubbles

will grow by creep of the fuel and/or coalescence of bubbles. Long operating time will probably result in bubbles large enough that surface energy effects may be neglected during most of the operating time. Therefore, the assumption is expected to be most applicable for long operating times, which is the major concern of this report.

Following reference 3, the fractional change in fuel volume caused by gaseous fission products x_g for a constant fission rate b/τ is given by

$$\left\{\int_0^{x_g} x_g^{n-1}\left[1-\left(\frac{x_g}{1+x_g}\right)^{1/n}\right]^n dx_g\right\}^{1/(n+1)} = \left[\frac{3a\tau}{2(n+1)}\left(\frac{3C_yKT_fNb}{n}\right)^n\right]^{1/(n+1)} \frac{t}{\tau} \qquad \text{(C23)}$$

Equation (C23) can be derived from the multiaxial creep equations of appendix B. This derivation, shown in appendix C, is included in this report for completeness. Equation (C23) is equivalent to the results of reference 3, except that in reference 3 x_g was assumed to be small compared to 1 and the term $(1 + x_g)$ does not appear.

Swelling caused by solid fission products is assumed, as in reference 2, to be directly proportional to the number of fissions based on atomic and molecular volumes. This assumption may be expressed as

$$x_s = \frac{C_s b t}{\tau} \qquad \text{(C24)}$$

The total change in fuel volume expressed as a fraction of the original volume is given by

$$x = x_g + x_s \qquad \text{(C25)}$$

The total volumetric swelling rate of the fuel is required for analysis of the plastic deformations in the fuel and clad cylinders. The engineering bulk strain rate for a constant fission rate is given by

$$\dot{x} = \dot{x}_g + \dot{x}_s \qquad \text{(C26)}$$

where $\dot{x}_g$ and $\dot{x}_s$ may be obtained from the derivatives of equations (C23) and (C24). Thus,

$$\dot{x}_g = \frac{\frac{3a}{2}\left(\frac{3C_y K T_f N b t}{n\tau}\right)^n}{x_g^{n-1}\left[1 - \left(\frac{x_g}{1 + x_g}\right)^{1/n}\right]^n} \tag{C22}$$

and

$$\dot{x}_s = C_s \frac{b}{\tau} \tag{C27}$$

The strain rates are more accurately expressed on the basis of true strain rather than engineering strain. The true bulk strain rate is related to the engineering bulk strain rate according to

$$\dot{v} = \frac{\dot{x}}{1 + x} \tag{B18}$$

and therefore

$$v = \ln(1 + x) \tag{B19}$$

The engineering strain rate $\dot{x}$ and the true strain rate v are essentially equal for small values of x.

Combining equation (B18) with equations (C25), (C26), (C22), and (C27) yields

$$\dot{v} = \left\{ \frac{\frac{3a}{2}\left(\frac{3C_y K T_f N b t}{n\tau}\right)^n}{x_g^{n-1}\left[1 - \left(\frac{x_g}{1 + x_g}\right)^{1/n}\right]^n} + C_s \frac{b}{\tau} \right\} \frac{1}{1 + x_g + C_s \frac{bt}{\tau}} \tag{C28}$$

Stresses and Strains in Fuel and Clad Cylinders

Equations for stress and strain in the fuel and clad cylinders are derived in appendix D. The derivation involves the following assumptions:

(1) The fuel and clad operate at uniform but possibly different temperatures; that is, radial temperature variations within the fuel and clad are neglected.

(2) The cylinders are long compared to their wall thickness, so that plane strain exists in the axial direction; that is, axial strain is independent of radius.

(3) The hydrostatic pressures at the inside surface of the fuel cylinder and the outside surface of the clad cylinder are zero.

(4) No axial force is transmitted between the fuel and clad cylinders.

Applying these assumptions, the tangential strain rate at the fuel-clad interface is given by the following equation from appendix D:

$$\alpha\left(\frac{3\dot{\epsilon}_{tm}}{\dot{v}}\right)^{n_f/n_c} + \frac{3\dot{\epsilon}_{tm}}{\dot{v}} - 1 = 0 \tag{D30}$$

where

$$\alpha \equiv \frac{a_f}{a_c^{n_f/n_c}} \left(\frac{3}{\dot{v}}\right)^{1-(n_f/n_c)} \left(\frac{\beta_c}{\beta_f}\right)^{n_f} \tag{D31}$$

Therefore, the parameter α determines the relative tangential strain rate at the fuel-clad interface ($3\dot{\epsilon}_{tm}/\dot{v}$).

The quantity β is a function only of the radius ratio φ_a or φ_b for a given value of n. Values of β have been calculated by numerical integration (see appendix D) and are shown plotted in figure 2 for several values of n.

The relative tangential strain rate at the fuel-clad interface ($3\dot{\epsilon}_{tm}/\dot{v}$) can be obtained from equations (D30) and (D31) and figure 2. All other strain rates can be determined from the following equations written in terms of the strain rate at the interface:

$$\dot{\epsilon}_t = \frac{\dot{v}}{3} - \frac{\left(\frac{\dot{v}}{3} - \dot{\epsilon}_{tm}\right)\left(1 + \frac{A\varphi^2}{\sqrt{3}}\right)}{\varphi^2\left(1 + \frac{A}{\sqrt{3}}\right)} \tag{D33}$$

$$\dot{\epsilon}_r = \frac{\dot{v}}{3} + \frac{\left(\frac{\dot{v}}{3} - \dot{\epsilon}_{tm}\right)\left(1 - \frac{A\varphi^2}{\sqrt{3}}\right)}{\varphi^2\left(1 + \frac{A}{\sqrt{3}}\right)} \tag{D34}$$

$$\dot{\epsilon}_z = \frac{\dot{v}}{3} + \frac{2A\left(\frac{\dot{v}}{3} - \dot{\epsilon}_{tm}\right)}{\sqrt{3}\left(1 + \frac{A}{\sqrt{3}}\right)} \tag{D35}$$

When applying these latter equations to the clad, $\dot{v}$ is taken to be zero. Values for the constant A have been calculated by numerical integration (see appendix D) and are shown plotted in figure 3.

The strain rates are, in general, functions of time and must be integrated with respect to t to obtain the strain in the time period from time zero to time t according to

$$\epsilon = \int_0^t \dot{\epsilon}\, dt \tag{D36}$$

It is desirable to express the strains as engineering strains to give a measure of the change in dimension relative to the original dimension. True strain ϵ can be converted to engineering strain δ according to the following relation from appendix B:

$$\delta = e^{\epsilon} - 1 \tag{B13}$$

RESULTS AND DISCUSSION

Strains in the fuel and clad of a nuclear reactor fuel pin caused by fuel swelling can be calculated from the equations developed in the appendixes and presented in the analysis. These equations and their application are discussed in the following sections.

Fuel Volumetric Swelling

The volumetric swelling of the fuel caused by gaseous fission products is given by equation (C23). This fractional change in volume x_g is seen to be a function of the fuel characteristics (N, a_f, and n_f), the design conditions (T, b, and τ), and the operating

time t. The solution to equation (C23), obtained by numerical integration, is presented in figure 4 for several values of n. The amount of swelling increases exponentially with time, and depending on the fuel and operating conditions can reach appreciable values. Volumetric swelling of the fuel caused by gaseous products should at least be limited to the point where the gas bubbles become interconnected leading to fission gas release from the fuel. Barnes (ref. 4) estimates that this point is reached at a volumetric swelling of $33\frac{1}{3}$ percent. Fuel swelling probably ceases at this point.

The amount of swelling given by equation (C23) and figure 4 is based on a particular swelling model. The model is subject to question, as would any model proposed on the basis of present knowledge. The fact that surface energy effects were neglected in the model implies that the analysis is not well suited to short-term irradiations when the fission gas bubbles are expected to be small. Neglecting surface energy effects is felt to be of minor consequence for long irradiation periods but leads to conservative designs for all cases. Swelling models which include surface tension must incorporate one or more additional assumptions not required here; namely, the mechanism of bubble coalescence and/or the bubble density. As better swelling models become available, they could be applied to the stress-strain analysis of the fuel and clad cylinders (appendix D) which is independent of the swelling model.

Swelling predictions of equation (C23) and figure 4 involve the assumption that volumetric swelling is unaffected by clad restraint. Actually, clad restraint would be expected to decrease the volumetric swelling of the fuel (see appendix C). However, the presence of a void space inside the fuel pin may allow the volumetric swelling of the fuel to approach the unrestrained swelling. In any case, the assumption used herein leads to a conservative design.

The amount of swelling depends on the fuel operating temperature, as can be seen from equation (C23). The fuel temperature T_f and the coefficient a in the creep rate equation (which is a function of temperature) both appear in equation (C23). The assumption of uniform fuel temperature could lead to significant errors where large temperature variations exist. Therefore, the analysis presented herein is not valid for such cases. Treatment of fuel pins where fuel swelling is a function of radius requires that the analysis be programmed for a digital computer and is beyond the scope of this report.

The amount of swelling caused by gaseous fission products increases with temperatures and is the major contribution to fuel swelling for high temperature applications. However, swelling caused by solid products is not negligible and its contribution (eq. (C24)) is included in the total swelling given by equation (C25).

Recent information obtained in the United Kingdom indicates that not all of the gaseous products participate in bubble growth because some of the gaseous products may exist in a supersaturated solid solution with the fuel material under irradiation conditions (ref. 6). This unexpected effect is also under investigation as part of the fuel swelling studies at the Battelle Memorial Research Institute (ref. 7). A knowledge of

the amount of this increased solubility could be incorporated in the present analysis by using a properly reduced value of C_y. Some evidence also exists to indicate that the creep strength of the fuel material under irradiation may be lower than that measured out-of-pile (ref. 7). This difference in creep strength has been attributed to local overheating of the fuel in the vicinity of the fission sites.

Strains in Fuel and Clad

The volumetric swelling rate $\dot{v}$ at any time t can be calculated from equation (C28) once the value of x_g at time t is known. The tangential strain rate at the fuel-clad interface may then be determined from equations (D30) and (D31) using figure 2 to obtain values for β in equation (D31). Equation (D30) is shown graphically in figure 5. The relative tangential strain rate ($3\dot{\epsilon}_{tm}/\dot{v}$) at the interface is a function of α and n_f/n_c. At small values of α (representing a strong fuel and a weak clad), the relative tangential strain rate approaches a value of 1. That is, the tangential strain rate is nearly the same as if the fuel were unrestrained and equal to one-third the volumetric swelling rate. At large values of α (representing a weak fuel and a strong clad) the relative strain rate approaches zero. That is, the clad strain rate is nil and the fuel is forced to strain axially and inward into the central void space if such a space exists. In between these two limits, as α approaches a value of 1, is a region where the strain rate is more sensitive to fractional changes in the value of α.

The value of α is dependent on the value of $\dot{v}$ which is a function of t. Therefore, the strain rate is also a function of t and, in general, must be integrated (either numerically or graphically) with respect to time to obtain the strain in the time period from time zero to time t, according to equation (D36). If, however, $\dot{v}$ does not vary greatly with t or if n_f/n_c is nearly equal to 1, then α will be insensitive to time. In such a case, the quantity $3\dot{\epsilon}_{tm}/\dot{v}$ will be nearly constant, and no time integration is necessary. The strain ϵ_{tm} at any time t for these cases may then be evaluated with little error from the values of $3\dot{\epsilon}_{tm}/\dot{v}$ and $v/3$ at time t as given by

$$\epsilon_{tm} = \left(\frac{3\dot{\epsilon}_{tm}}{\dot{v}}\right)\left(\frac{v}{3}\right) = \left(\frac{3\dot{\epsilon}_{tm}}{\dot{v}}\right)\left[\frac{\ln\left(1 + x_g + \frac{C_s bt}{\tau}\right)}{3}\right]$$

The magnitude of the error introduced by this equation obviously depends on the variation in the value of $3\dot{\epsilon}_{tm}/\dot{v}$ with time and may be evaluated from the following

$$\epsilon_{tm} = \int_0^t \dot{\epsilon}_{tm}\, dt = \int_0^t \left(\frac{3\dot{\epsilon}_{tm}}{\dot{v}}\right)\frac{\dot{v}}{3}\,dt = \left(\frac{3\dot{\epsilon}_{tm}}{\dot{v}}\right)\frac{v}{3} - \int_0^t \frac{v}{3}\frac{d}{dt}\left(\frac{3\dot{\epsilon}_{tm}}{\dot{v}}\right) dt$$

Thus, if $3\dot{\epsilon}_{tm}/\dot{v}$ is constant, the second term is zero. If $3\dot{\epsilon}_{tm}/\dot{v}$ varies with time, the maximum error introduced by neglecting the second term is

$$\frac{v_{max}}{3}\left[\left(\frac{3\dot{\epsilon}_{tm}}{\dot{v}}\right) - \left(\frac{3\dot{\epsilon}_{tm}}{\dot{v}}\right)_{t=0}\right]$$

Because v increases with time, the maximum value of v occurs at time t and the maximum error introduced by neglecting the second term is

$$\frac{v}{3}\left[\left(\frac{3\dot{\epsilon}_{tm}}{\dot{v}}\right) - \left(\frac{3\dot{\epsilon}_{tm}}{\dot{v}}\right)_{t=0}\right]$$

Strain rates at other locations in the fuel and clad cylinders may be calculated from equations (D33), (D34), and (D35) using figure 3 to obtain values for A. Again, if $\dot{v}$ does not vary greatly with t or if n_f/n_c is nearly equal to 1, no time integration is necessary, and the strain at any time t may be evaluated from

$$\epsilon = \left(\frac{\dot{\epsilon}}{\dot{\epsilon}_{tm}}\right)(\epsilon_{tm})$$

A conventional form of the creep rate equation was used in the analysis. There are limits which should be imposed on any equation of this form for practical materials. Limits on strain are obviously necessary because every material will ultimately rupture. Most designs will have strain limits on diametrical swelling of the clad dictated by other considerations, such as heat transfer. Limits on stress may also be necessary to restrict the range over which any one creep rate equation applies. It may therefore be advisable, if high stress levels are suspected, to check the stress level using equations of appendix D and choose a strain rate equation in accordance with the calculated value of stress.

The equations resulting from the analysis which predict the creep rates in the fuel and clad are independent of fuel pin size. Creep rates are seen to be functions of terms which are entirely dependent on dimensionless parameters defining the operating conditions, material properties, and radius ratios.

Although the assumptions used herein restrict the analysis to special cases, the results show the relative importance of operating conditions and material creep properties for these cases and give some insight as to their effect for other situations. The assumption of uniform temperature in the fuel and clad can never be achieved in practice and can only be approached with small diameter fuel pins, high thermal conductivity materials, and low burnup rates. Reactor applications requiring long operating lifetimes, such as space power systems, imply low burnup rates. These are the applications of most interest here. Such applications coupled with a fuel of high thermal conductivity will operate with a small temperature drop across the fuel. Other reactor applications which operate with a large temperature drop across the fuel and/or large variations in burnup across the fuel require that the analysis be programmed for a digital computer.

Numerical Example

A numerical example is presented to illustrate use of the equations and graphs and also to illustrate typical results obtained from the analysis. The following inputs were selected for this example:

Absolute fuel temperature, T_f, K	1500
Coefficient in equation (B4), for fuel, a_f, $\left(N/cm^2\right)^{-n_f}$ (hr^{-1})	1.026×10^{-18}
Exponent on stress in equation (B4), for fuel, n_f	4.0
Total uranium atoms per unit volume of fuel material, N, atoms/cm^3	3.3×10^{22}
Fractional change in atomic or molecular volume of solids occurring as result of fission, C_s	1.2
Absolute clad temperature, T_c, K	1400
Coefficient in equation (B4), for clad, a_c, $\left(N/cm^2\right)^{-n_c}$ (hr^{-1})	3.34×10^{-20}
Exponent on stress in equation (B4), for clad, n_c	3.7
Fraction of fission products in gaseous state, C_y	0.125
Boltzmann constant, K, N-cm/K-mol	1.381×10^{-21}
Burnup fraction, b	0.03
Total irradiation time to achieve burnup fraction b, τ, hr	20 000
Fuel radius ratio, φ_a	0.3
Clad radius ratio, φ_b	1.2

The volumetric swelling caused by gaseous fission products x_g may be obtained from figure 4. The value of the abscissa in figure 4 is

$$\left[\frac{3\times1.026\times10^{-18}\times 20\ 000}{2(4+1)}\left(\frac{3\times0.125\times1.381\times10^{-21}\times1500\times3.30\times10^{22}\times0.03}{4}\right)^4\right]^{1/(4+1)}$$

$$\times\frac{t}{\tau} = 0.0965\,\frac{t}{\tau}$$

The values of t/τ at various values of time t are given in table I along with the values of x_g read from figure 4.

The volumetric strain rate of the fuel is calculated from equation (C28). For example, at $t = 10\ 000$ hours,

$$\dot{v} = \frac{\dfrac{3\times1.026\times10^{-18}}{2}\left(\dfrac{3\times0.125\times1.381\times10^{-21}\times1500\times3.30\times10^{22}\times0.03\times10\ 000}{4\times20\ 000}\right)^4 + \dfrac{1.2\times0.03}{20\ 000}}{0.059^{4-1}\left[1-\left(\dfrac{0.059}{1+0.059}\right)^{1/4}\right]^4}$$

$$1 + 0.059 + \frac{(1.2)(0.03)(10\ 000)}{20\ 000}$$

$$= 1.02\times10^{-5}$$

Values of β are obtained from figure 2:

$$\beta_f = 0.794 \qquad \text{at } \varphi_a = 0.3 \text{ and } n_f = 4$$

$$\beta_c = 0.159 \qquad \text{at } \varphi_b = 1.2 \text{ and } n_c = 3.7$$

Values of α are computed from equation (D31). For example, at $t = 10\ 000$ hours,

$$\alpha = \frac{1.026\times10^{-18}}{\left(3.34\times10^{-20}\right)^{4/3.7}}\left(\frac{3}{1.02\times10^{-5}}\right)^{1-(4/3.7)}\left(\frac{0.159}{0.794}\right)^4 = 0.727$$

The relative tangential strain rate at the fuel-clad interface $3\dot{\epsilon}_{tm}/\dot{v}$ is read from figure 5 or calculated from equation (D30), as given in column 6 of table I. The tangential strain rate at the interface is

$$\dot{\epsilon}_{tm} = \left(\frac{3\dot{\epsilon}_{tm}}{\dot{v}}\right)\frac{\dot{v}}{3}$$

For example, at t = 10 000 hours,

$$\dot{\epsilon}_{tm} = 0.593\left(\frac{1.02\times10^{-5}}{3}\right) = 2.02\times10^{-6}\ \text{hr}^{-1}$$

Other strain rates are calculated from equations (D33), (D34), and (D35), noting that for the clad ($1 < \varphi < \varphi_b$) $\dot{v}$ is taken to be zero. For example, $A_c = 0.397$ (from fig. 3(b)), then at t = 10 000 hours,

$$\dot{\epsilon}_{tb} = 0 - \frac{(0 - 2.02\times10^{-6})\left(1 + \frac{0.397\times1.2^2}{\sqrt{3}}\right)}{1.2^2\left(1 + \frac{0.397}{\sqrt{3}}\right)} = 1.52\times10^{-6}\ \text{hr}^{-1}$$

The strain rates at various positions in the fuel and clad vary with time. The true tangential strain rate at the fuel-clad interface $\dot{\epsilon}_{tm}$ is shown in figure 6 as a function of time. Integrating this function from time zero to time t either numerically or graphically yields the strain at any time t (eq. (D36)). For this numerical example, $3\dot{\epsilon}_{tm}/\dot{v}$ does not vary greatly with time (see table I). Therefore, no time integration is necessary, and the approximate equations given in the section RESULTS AND DISCUSSION are applicable. Thus, at t = 10 000 hours,

$$\epsilon_{tm} = \left(\frac{3\dot{\epsilon}_{tm}}{\dot{v}}\right)\frac{\ln\left(1 + x_g + \frac{C_s bt}{\tau}\right)}{3} = \frac{0.593}{3}\ln\left[1 + 0.059 + (1.2)(0.03)(0.5)\right] = 0.015$$

Engineering tangential strain is then determined from equation (B13)

$$\delta_{tm} = e^{0.015} - 1 = 0.015$$

Engineering tangential strain as a function of time is shown in table I and in figure 7 for three locations: the fuel-clad interface, the clad outside radius, and the fuel inside

radius. The axial strains δ_z for the fuel and clad are also shown. All of the strains increase monotonically with time. It can be seen that the clad increases in diameter at both its inside and outside surfaces, whereas the fuel increases in diameter at its outside surface but decreases in diameter at its inside surface. The tangential strain in the clad is highest at its inside surface and equal to 4.1 percent at the end of the assumed life. The change in outside diameter of the clad is 3.0 percent at the end of life.

The axial strain in the fuel is the largest of all the strains. The fuel increases in length by 11.4 percent. The clad decreases in length by 1.5 percent. In order to accommodate the relative axial expansion of fuel and clad, an axial void space of at least 12.9 percent of the fuel length must be provided.

Lewis Research Center,
National Aeronautics and Space Administration,
Cleveland, Ohio, October 8, 1969,
120-27.

APPENDIX A

SYMBOLS

A	grouping of constants defined by eq. (D13)
a	coefficient in creep rate equation (eq. (B4))
B	grouping of constants defined by eq. (D17)
b	burnup fraction, fraction of total uranium atoms fissioned in total time τ
C_1, C_2	constants of integration
C_s	fractional change in atomic or molecular volume of solids occurring as result of fission
C_y	fraction of fission products in gaseous state
K	Boltzmann constant
l	arbitrary length
N	total uranium atoms per unit volume of fuel material
n	exponent on stress in creep rate equation (eq. (B4))
p	pressure
r	radius
T	absolute temperature
t	time
$\dot{u}$	rate at which an incremental radius dr is changing
V	fuel volume at any time t
v	true bulk strain caused by solid and gaseous fission products, defined by eq. (B17)
$\dot{v}$	true bulk strain rate caused by solid and gaseous fission products, defined by eq. (B15)
x	fractional fuel volume change caused by solid and gaseous fission products, engineering bulk strain defined by eq. (B16)
$\dot{x}$	fractional fuel volumetric swelling rate caused by solid and gaseous fission products, engineering bulk strain rate defined by eq. (B14)
x_g	fractional fuel volume change caused by gaseous fission products
$\dot{x}_g$	fractional fuel volumetric swelling rate caused by gaseous fission products
x_s	fractional fuel volume change caused by solid fission products
$\dot{x}_s$	fractional fuel volumetric swelling rate caused by solid fission products
α	defined by eq. (D31)
β	defined by eq. (D32)
γ	defined by eq. (B1)

δ	engineering strain, defined by eq. (B11)
$\dot{\delta}$	engineering strain rate, defined by eq. (B9)
ϵ	true strain, defined by eq. (B12)
$\dot{\epsilon}$	true strain rate, defined by eq. (B10)
$\dot{\epsilon}^*$	effective multiaxial unit strain rate
σ	stress
σ^*	effective multiaxial stress
τ	total irradiation time to achieve burnup fraction b
φ	radius ratio, r/r_m

Subscripts:

a	inner radius of fuel cylinder
b	outer radius of clad cylinder
c	clad
f	fuel
i	inner radius of fuel sphere (gas bubble radius)
m	reference radius, radius at fuel-clad interface ($\varphi = 1$)
o	outer radius of fuel sphere
r	radial
t	tangential
z	axial
0	original value at $t = 0$
1, 2, 3	components in triaxial stress condition

APPENDIX B

MULTIAXIAL CREEP EQUATIONS

The analytical treatment of steady-state creep under multiaxial stress appears in the literature (e.g., ref. 5). The relation between stress and strain rates in this prior treatment is based on the assumption that at any point in a stressed body the principal shear strain rates are proportional to the principal shear stresses

$$\frac{\dot{\epsilon}_1 - \dot{\epsilon}_2}{\sigma_1 - \sigma_2} = \frac{\dot{\epsilon}_2 - \dot{\epsilon}_3}{\sigma_2 - \sigma_3} = \frac{\dot{\epsilon}_3 - \dot{\epsilon}_1}{\sigma_3 - \sigma_1} \equiv \gamma \tag{B1}$$

where $\dot{\epsilon}$ is the strain rate, σ is the stress, γ is a proportionality factor to be evaluated, and the subscripts 1, 2, and 3 refer to the three mutually perpendicular strain axes in a multiaxial system.

The sum of the strain rates is equal to the rate of change in volume. Therefore,

$$\dot{\epsilon}_1 + \dot{\epsilon}_2 + \dot{\epsilon}_3 = \dot{v} \tag{B2}$$

The change in volume of a solid under plastic deformation is usually taken to be zero ($\dot{v} = 0$). The more general form (eq. (B2)) is used herein so that it can be applied to the fuel cylinder (solid plus gas bubbles) which is increasing in volume as fission products are generated.

Combining equations (B1) and (B2) yields

$$\dot{\epsilon}_1 = \frac{\dot{v}}{3} + \frac{\gamma}{3}(2\sigma_1 - \sigma_2 - \sigma_3) \tag{B3a}$$

$$\dot{\epsilon}_2 = \frac{\dot{v}}{3} + \frac{\gamma}{3}(2\sigma_2 - \sigma_3 - \sigma_1) \tag{B3b}$$

$$\dot{\epsilon}_3 = \frac{\dot{v}}{3} + \frac{\gamma}{3}(2\sigma_3 - \sigma_1 - \sigma_2) \tag{B3c}$$

A creep rate equation of the following form is assumed for a given temperature in a multiaxial system

$$\dot{\epsilon}^* = a\sigma^{*n} \tag{B4}$$

where the effective stress and strain based on distortion energy are defined by

$$\dot{\epsilon}^* = \frac{\sqrt{2}}{3}\left[\left(\dot{\epsilon}_1 - \dot{\epsilon}_2\right)^2 + \left(\dot{\epsilon}_2 - \dot{\epsilon}_3\right)^2 + \left(\dot{\epsilon}_3 - \dot{\epsilon}_1\right)^2\right]^{1/2} \tag{B5}$$

$$\sigma^* = \frac{1}{\sqrt{2}}\left[\left(\sigma_1 - \sigma_2\right)^2 + \left(\sigma_2 - \sigma_3\right)^2 + \left(\sigma_3 - \sigma_1\right)^2\right]^{1/2} \tag{B6}$$

The quantity γ in equation (B3) is determined from a uniaxial stress condition by setting $\sigma_2 = \sigma_3 = 0$. Then, $\dot{\epsilon}_2 = \dot{\epsilon}_3$, and equations (B2), (B5), and (B6) reduce to

$$\dot{\epsilon}_2 = \frac{\dot{v}}{2} - \frac{\dot{\epsilon}_1}{2}$$

$$\dot{\epsilon}^* = \dot{\epsilon}_1 - \frac{\dot{v}}{3}$$

$$\sigma^* = \sigma_1$$

Applying this uniaxial stress condition to equation (B3a) and substituting from equation (B4) yields

$$\gamma = \frac{3a}{2}\sigma^{*n-1} \tag{B7}$$

Combining equations (B3) and (B7) yields

$$\dot{\epsilon}_1 = \frac{\dot{v}}{3} + \frac{a\sigma^{*n-1}}{2}\left(2\sigma_1 - \sigma_2 - \sigma_3\right) \tag{B8a}$$

$$\dot{\epsilon}_2 = \frac{\dot{v}}{3} + \frac{a\sigma^{*n-1}}{2}\left(2\sigma_2 - \sigma_3 - \sigma_1\right) \tag{B8b}$$

$$\dot{\epsilon}_3 = \frac{\dot{v}}{3} + \frac{a\sigma^{*n-1}}{2}\left(2\sigma_3 - \sigma_1 - \sigma_2\right) \tag{B8c}$$

Thus, equation (B8) is the relation between stress and strain in a multiaxial system.

The foregoing equations are strictly applicable for true strain rates. It is desirable, however, to express the strains as engineering strains to give a measure of the change in length or volume relative to the original values. Defining engineering strain rate as

$$\dot{\delta} = \frac{dl}{l_0\, dt} \tag{B9}$$

and true strain rate as

$$\dot{\epsilon} = \frac{dl}{l\, dt} \tag{B10}$$

then the engineering strain is given by

$$\delta = \int_{l_0}^{l} \frac{dl}{l_0} = \frac{l - l_0}{l_0} \tag{B11}$$

and the true strain is given by

$$\epsilon = \int_{l_0}^{l} \frac{dl}{l} = \ln \frac{l}{l_0} \tag{B12}$$

Therefore, the engineering and true strains are related according to

$$\epsilon = \ln(1 + \delta)$$

or

$$\delta = e^{\epsilon} - 1 \tag{B13}$$

Similarly, the bulk strain rates are defined as

$$\dot{x} = \frac{dV}{V_0\, dt} \tag{B14}$$

$$\dot{v} = \frac{dV}{V\, dt} \tag{B15}$$

Therefore,

$$x = \frac{V - V_0}{V_0} \tag{B16}$$

$$v = \ln \frac{V}{V_0} \tag{B17}$$

and

$$\dot{v} = \frac{\dot{x}}{1 + x} \tag{B18}$$

$$v = \ln(1 + x) \tag{B19}$$

APPENDIX C

FUEL SWELLING

The analysis for fuel swelling caused by fission gas containment in the fuel follows that given in reference 3. The calculational model reduces the fuel swelling problem to a determination of the creep of an internally pressurized thick-walled sphere. The multiaxial creep equations of appendix B can be applied to a sphere by making the following substitutions

$$\sigma_1 = \sigma_2 = \sigma_t$$

$$\sigma_3 = \sigma_r$$

$$\dot{\epsilon}_1 = \dot{\epsilon}_2 = \dot{\epsilon}_t$$

$$\dot{\epsilon}_3 = \dot{\epsilon}_r$$

Because of the symmetry of components 1 and 2, equations (B5) and (B6) reduce to

$$\sigma^* = \sigma_t - \sigma_r \tag{C1}$$

$$\dot{\epsilon}^* = \frac{2}{3}(\dot{\epsilon}_t - \dot{\epsilon}_r) \tag{C2}$$

It is assumed that the volume of the solid does not change during plastic deformation ($\dot{v} = 0$). This condition of incompressibility reduces equation (B2) to

$$2\dot{\epsilon}_t = -\dot{\epsilon}_r \tag{C3}$$

Combining equations (C2) and (C3),

$$\dot{\epsilon}^* = 2\dot{\epsilon}_t \tag{C4}$$

The strain rates in spherical geometry are given by

$$\dot{\epsilon}_r = \frac{d\dot{u}}{dr} \tag{C5}$$

$$\dot{\epsilon}_t = \frac{\dot{u}}{r} \tag{C6}$$

where $\dot{u}$ is the rate at which an incremental radius dr is changing.

Substituting from equations (C3) and (C6) into equation (C5) and integrating,

$$\dot{u} = \frac{C_1}{r^2} \tag{C7}$$

Combining equations (C4), (C6), and (C7),

$$\dot{\epsilon}^* = \frac{2C_1}{r^3} \tag{C8}$$

The equilibrium equation for a sphere is

$$r \frac{d\sigma_r}{dr} = 2(\sigma_t - \sigma_r) \tag{C9}$$

Combining equations (B4), (C1), (C8), and (C9),

$$\frac{d\sigma_r}{dr} = 2\left(\frac{2C_1}{a}\right)^{1/n} r^{-3/(n-1)} \tag{C10}$$

Integrating equation (C10),

$$\sigma_r = -\frac{2n}{3}\left(\frac{2C_1}{a}\right)^{1/n}\left(\frac{1}{r}\right)^{3/n} + C_2 \tag{C11}$$

The boundary condition at the inside and outside surfaces of the sphere are

$$\sigma_{ri} = -p_i$$

$$\sigma_{ro} = -p_o$$

Applying these boundary conditions to equation (C11),

$$\sigma_r = \frac{(p_i - p_o)\left[\left(\frac{r_o}{r_i}\right)^{3/n} - \left(\frac{r_o}{r}\right)^{3/n}\right]}{\left(\frac{r_o}{r_i}\right)^{3/n} - 1} - p_i \tag{C12}$$

Differentiating equation (C12),

$$\frac{d\sigma_r}{dr} = \frac{3(p_i - p_o)\left(\frac{r_o}{r}\right)^{3/n}}{nr\left[\left(\frac{r_o}{r_i}\right)^{3/n} - 1\right]} \tag{C13}$$

Combining equations (B4), (C2), (C4), (C9), and (C13),

$$\dot{\epsilon}_t = \frac{a}{2}\left[\frac{\frac{3}{2n}(p_i - p_o)\left(\frac{r_o}{r}\right)^{3/n}}{\left(\frac{r_o}{r_i}\right)^{3/n} - 1}\right]^n$$

Then at $r = r_i$

$$\dot{\epsilon}_{ti} = \frac{dr_i}{r_i\, dt} = \frac{a}{2}\left[\frac{\frac{3}{2n}(p_i - p_o)}{1 - \left(\frac{r_i}{r_o}\right)^{3/n}}\right]^n \tag{C14}$$

The radii in equation (C14) can be written in terms of volume ratios. Let x_g denote the fractional fuel volume change caused by gaseous fission products, that is, the gas volume expressed as a fraction of the original fuel volume. Then,

$$x_g = \frac{\frac{4}{3}\pi r_i^3}{V_0} \tag{C15}$$

and

$$\frac{dx_g}{dt} = \frac{3x_g}{r_i}\frac{dr_i}{dt} \tag{C16}$$

The solid fuel volume is assumed here to be constant with respect to time and equal to the original fuel volume. Therefore,

$$\frac{4}{3}\pi\left(r_o^3 - r_i^3\right) = V_0 \tag{C17}$$

and combining with equation (C15) yields

$$\frac{r_i^3}{r_o^3} = \frac{x_g}{1 + x_g} \tag{C18}$$

Substituting equations (C17) and (C18) into equation (C14) yields

$$\left[1 - \left(\frac{x_g}{1 + x_g}\right)^{1/n}\right]^n \frac{dx_g}{x_g} = \frac{3a}{2}\left[\frac{3p_i}{2n}\left(1 - \frac{p_o}{p_i}\right)\right]^n dt \tag{C19}$$

Assuming the gaseous fission products to be ideal gases

$$p_i = \frac{2C_y K T_f N b t}{x_g \tau} \tag{C20}$$

Combining equations (C19) and (C20)

$$\dot{x}_g = \frac{\frac{3a}{2}\left[\frac{3C_y K T_f N b t}{n\tau}\left(1 - \frac{p_o}{p_i}\right)\right]^n}{x_g^{n-1}\left[1 - \left(\frac{x_g}{1 + x_g}\right)^{1/n}\right]^n} \tag{C21}$$

A pressure p_o at the outside surface of the sphere could be produced as a result of a constraint at the outside of the fuel body. In order to simplify the problem and yield a conservative design, the pressure p_o is taken to be zero. Equation (C21) then becomes

$$\dot{x}_g = \frac{\frac{3a}{2}\left(\frac{3C_y K T_f N b t}{n\tau}\right)^n}{x_g^{n-1}\left[1 - \left(\frac{x_g}{1 + x_g}\right)^{1/n}\right]^n} \tag{C22}$$

Equation (C22) will therefore yield a volumetric swelling rate corresponding to an unrestrained condition which will be greater than the expected swelling rate if a clad is present to make p_o greater than zero.

Integrating equation (C22) between the limits from zero to x_g and zero to t, for a constant fission rate b/τ, yields

$$\left\{\int_0^{x_g} x_g^{n-1}\left[1 - \left(\frac{x_g}{1 + x_g}\right)^{1/n}\right]^n dx_g\right\}^{1/(n+1)} = \left[\frac{3a\tau}{2(n+1)}\left(\frac{3C_y K T_f N b}{n}\right)^n\right]^{1/(n+1)} \frac{t}{\tau} \tag{C23}$$

Equation (C23) is equivalent to the results of reference 3, except that in reference 3, x_g was assumed to be small compared to 1 and the term $(1 + x_g)$ does not appear.

The swelling caused by solid fission products is assumed, as in reference 2, to be directly proportional to the number of fissions. This assumption is based on atomic or molecular volumes originally proposed in reference 8. Solid fission product swelling is then expressed as

$$x_s = \frac{C_s b t}{\tau} \tag{C24}$$

where the constant C_s is the fractional change in atomic or molecular volume of solids occurring as a result of fission. The value of C_s depends on the fuel compound.

The total change in fuel volume expressed as a fraction of the original volume is

$$x = x_g + x_s \tag{C25}$$

The engineering bulk strain rate is then

$$\dot{x} = \dot{x}_g + \dot{x}_s \tag{C26}$$

where for a constant fission rate $\dot{x}_g$ is given by equation (C22) and $\dot{x}_s$ is obtained by differentiating equation (C24) with respect to time.

$$\dot{x}_s = C_s \frac{b}{\tau} \tag{C27}$$

The true bulk strain rate may then be determined from equation (B18). Substituting equations (C22), (C25), (C26), and (C27) into equation (B18) yields

$$\dot{v} = \left\{ \frac{\frac{3a}{2}\left(\frac{3C_y K T_f N b t}{n\tau}\right)^n}{x_g^{n-1}\left[1 - \left(\frac{x_g}{1+x_g}\right)^{1/n}\right]^n} + C_s \frac{b}{\tau} \right\} \frac{1}{1 + x_g + \frac{C_s b t}{\tau}} \tag{C28}$$

Equation (C28) gives the true bulk strain rate of the fuel for a constant fission rate based on the calculational model assumed herein.

APPENDIX D

CREEP ANALYSIS FOR FUEL AND CLAD CYLINDERS

Stress and strain in the fuel and clad cylinders can be analyzed using the general equations of appendix B and the volumetric fuel swelling equations of appendix C. Equations (B2), (B5), (B6), and (B8) can be written in polar coordinates for application to cylindrical geometry as follows

$$\dot{\epsilon}_z + \dot{\epsilon}_t + \dot{\epsilon}_r = \dot{v} \tag{D1}$$

$$\dot{\epsilon}^* = \frac{\sqrt{2}}{3}\left[\left(\dot{\epsilon}_z - \dot{\epsilon}_t\right)^2 + \left(\dot{\epsilon}_t - \dot{\epsilon}_r\right)^2 + \left(\dot{\epsilon}_r - \dot{\epsilon}_z\right)^2\right]^{1/2} \tag{D2}$$

$$\sigma^* = \frac{1}{\sqrt{2}}\left[\left(\sigma_z - \sigma_t\right)^2 + \left(\sigma_t - \sigma_r\right)^2 + \left(\sigma_r - \sigma_z\right)^2\right]^{1/2} \tag{D3}$$

$$\dot{\epsilon}_z = \frac{\dot{v}}{3} + \frac{a\sigma^{*n-1}}{2}\left(2\sigma_z - \sigma_t - \sigma_r\right) \tag{D4a}$$

$$\dot{\epsilon}_t = \frac{\dot{v}}{3} + \frac{a\sigma^{*n-1}}{2}\left(2\sigma_t - \sigma_r - \sigma_z\right) \tag{D4b}$$

$$\dot{\epsilon}_r = \frac{\dot{v}}{3} + \frac{a\sigma^{*n-1}}{2}\left(2\sigma_r - \sigma_z - \sigma_t\right) \tag{D4c}$$

It is assumed that the cylinder is long compared to its diameter so that plane strain exists in the axial direction. Therefore, $\dot{\epsilon}_z$ is independent of the radius. Consequently, $d\dot{\epsilon}_z/dr = 0$ and $\dot{\epsilon}_z = C_1$.

Applying this restriction, equations (D1), (D2), and (D4a) become

$$C_1 + \dot{\epsilon}_t + \dot{\epsilon}_r = \dot{v} \tag{D5}$$

$$\dot{\epsilon}^* = \frac{\sqrt{2}}{3}\left[\left(C_1 - \dot{\epsilon}_t\right)^2 + \left(\dot{\epsilon}_t - \dot{\epsilon}_r\right)^2 + \left(\dot{\epsilon}_r - C_1\right)^2\right]^{1/2} \tag{D6}$$

$$C_1 = \frac{\dot{v}}{3} + \frac{a\sigma^{*n-1}}{2}(2\sigma_z - \sigma_t - \sigma_r) \tag{D7}$$

The compatibility equation (ref. 5) is expressed as

$$r\frac{d\dot{\epsilon}_t}{dr} = \dot{\epsilon}_r - \dot{\epsilon}_t \tag{D8}$$

Combining equations (D5) and (D8) and integrating,

$$\dot{\epsilon}_t = \frac{\dot{v} - C_1}{2} - \frac{C_2}{r^2}$$

Let

$$\varphi \equiv \frac{r}{r_m} \tag{D9}$$

where r_m is a reference radius. Then,

$$\dot{\epsilon}_t = \frac{\dot{v} - C_1}{2} - \frac{C_2}{r_m^2\varphi^2} \tag{D10}$$

Combining equations (D5) and (D10),

$$\dot{\epsilon}_r = \frac{\dot{v} - C_1}{2} + \frac{C_2}{r_m^2\varphi^2} \tag{D11}$$

Combining equations (D6), (D10), and (D11),

$$\dot{\epsilon}^* = \frac{2C_2}{\sqrt{3}\, r_m^2\varphi^2}\left(1 + A^2\varphi^4\right)^{1/2} \tag{D12}$$

where A is defined as

$$A \equiv \frac{(3C_1 - \dot{v})r_m^2}{2\sqrt{3}\, C_2} \tag{D13}$$

Combining equations (B4) and (D12)

$$\sigma^* = \left(\frac{2C_2 \sqrt{1 + A^2\varphi^4}}{\sqrt{3}\, r_m^2 \varphi^2 a} \right)^{1/n} \tag{D14}$$

The equilibrium equation (ref. 5) is

$$r \frac{d\sigma_r}{dr} = \sigma_t - \sigma_r$$

or using the definition of φ (eq. (D9))

$$\varphi \frac{d\sigma_r}{d\varphi} = \sigma_t - \sigma_r \tag{D15}$$

Combining equations (D4b), (D4c), and (D15),

$$\varphi \frac{d\sigma_r}{d\varphi} = \frac{2}{3a\sigma^{*n-1}} (\dot{\epsilon}_t - \dot{\epsilon}_r)$$

Combining this equation with equations (D10), (D11), and (D14) gives the radial stress gradient

$$\frac{d\sigma_r}{d\varphi} = \frac{-B}{\left(1 + A^2\varphi^4\right)^{(n-1)/2n} \varphi^{(n+2)/n}} \tag{D16}$$

where B is defined as

$$B \equiv \left(\frac{2^{n+1} C_2}{3^{(n+1)/2} a r_m^2} \right)^{1/n} \tag{D17}$$

The radial stress can be determined from equation (D16) and the boundary conditions which are discussed later in this appendix.

The tangential stress may be obtained from the equilibrium equation (eq. (D15)) and equation (D16)

$$\sigma_t = \sigma_r - \frac{B}{\left(1 + A^2\varphi^4\right)^{(n-1)/2n} \varphi^{2/n}} \tag{D18}$$

The axial stress may be obtained by combining equations (D17), (D14), and (D18) using the definitions of A and B (eqs. (D13) and (D17))

$$\sigma_z = \sigma_r + \frac{B\left(A\sqrt{3}\,\varphi^2 - 1\right)}{2\left(1 + A^2\varphi^4\right)^{(n-1)/2n} \varphi^{2/n}} \tag{D19}$$

The tangential and radial strain rates are given by equations (D1) and (D11) in combination with equations (D13) and (D17)

$$\dot{\epsilon}_t = \frac{\dot{v}}{3} - \frac{a3^{(n+1)/2}}{2^{(n+1)}\varphi^2} B^n \left(1 + \frac{A\varphi^2}{\sqrt{3}}\right) \tag{D20a}$$

$$\dot{\epsilon}_r = \frac{\dot{v}}{3} + \frac{a3^{(n+1)/2}}{2^{n+1}\varphi^2} B^n \left(1 - \frac{A\varphi^2}{\sqrt{3}}\right) \tag{D20b}$$

Boundary Conditions

The boundary conditions can be specified in terms of the radial stress at the inside and outside surfaces of the fuel and clad cylinders, the axial force on the cylinders, and the tangential strain rate at the interface of the fuel and clad.

The pressure at the inside surface of the fuel cylinder and the outside surface of the clad cylinder is taken to be zero. Also the fuel and clad cylinders have a common contact pressure p_m at their interface. Therefore, from the definition of φ (eq. (D9))

$$\sigma_r = 0 \qquad \text{at} \quad \varphi = \frac{r_a}{r_m} = \varphi_a$$

$$\sigma_r = 0 \qquad \text{at} \quad \varphi = \frac{r_b}{r_m} = \varphi_b$$

$$\sigma_r = -p_m \qquad \text{at} \quad \varphi = 1$$

where r_a is the inner radius of the fuel cylinder, r_b is the outer radius of the clad cylinder, and the reference radius r_m is taken to be the radius at the fuel-clad interface. Applying these conditions to equation (D16) and integrating yields

$$\sigma_r = B_f \int_{\varphi}^{\varphi_a} \frac{d\varphi}{\left(1 + A_f^2 \varphi^4\right)^{(n-1)/2n} \varphi^{(n+2)/n}} \tag{D21}$$

$$\sigma_r = B_c \int_{\varphi}^{\varphi_b} \frac{d\varphi}{\left(1 + A_c^2 \varphi^4\right)^{(n-1)/2n} \varphi^{(n+2)/n}} \tag{D22}$$

$$\frac{p_m}{B_f} = \int_{\varphi_a}^{1} \frac{d\varphi}{\left(1 + A_f^2 \varphi^4\right)^{(n-1)/2n} \varphi^{(n+2)/n}} \tag{D23}$$

$$\frac{p_m}{B_c} = \int_{\varphi_b}^{1} \frac{d\varphi}{\left(1 + A_c^2 \varphi^4\right)^{(n-1)/2n} \varphi^{(n+2)/n}} \tag{D24}$$

It is assumed that no axial force is transmitted between the fuel and clad cylinders. Therefore, the net axial force on the cylinders is zero, or

$$\int_{\varphi_a}^{1} \sigma_z \varphi \, d\varphi = 0$$

$$\int_{\varphi_b}^{1} \sigma_z \varphi \, d\varphi = 0$$

Applying these conditions to equations (D19), (D21), and (D22),

$$\int_{\varphi_a}^{1}\left[\int_{\varphi}^{\varphi_a}\frac{d\varphi}{\left(1+A_f^2\varphi^4\right)^{(n-1)/2n}\varphi^{(n+2)/n}}+\frac{A_f\sqrt{3}\,\varphi^2-1}{2\left(1+A_f^2\varphi^4\right)^{(n-1)/2n}\varphi^{2/n}}\right]\varphi\,d\varphi=0 \qquad \text{(D25)}$$

$$\int_{\varphi_b}^{1}\left[\int_{\varphi}^{\varphi_b}\frac{d\varphi}{\left(1+A_c^2\varphi^4\right)^{(n-1)/2n}\varphi^{(n+2)/n}}+\frac{A_c\sqrt{3}\,\varphi^2-1}{2\left(1+A_c^2\varphi^4\right)^{(n-1)/2n}\varphi^{2/n}}\right]\varphi\,d\varphi=0 \qquad \text{(D26)}$$

The tangential strain rates of the fuel and clad must be equal at their interface because they are in contact. Therefore, applying equation (D20) to the fuel and clad cylinders at their interface ($\varphi = 1$),

$$\dot{\epsilon}_{tm}=\frac{\dot{v}}{3}-\frac{a_f{}^{3^{(n_f+1)/2}}}{2^{n_f+1}}\left(\frac{B_f}{p_m}\right)^{n_f}\left(1+\frac{A_f}{\sqrt{3}}\right)\left(p_m\right)^{n_f} \qquad \text{(D27)}$$

$$\dot{\epsilon}_{tm}=\frac{a_c{}^{3^{(n_c+1)/2}}}{2^{n_c+1}}\left(-\frac{B_c}{p_m}\right)^{n_c}\left(1+\frac{A_c}{\sqrt{3}}\right)\left(p_m\right)^{n_c} \qquad \text{(D28)}$$

When applying equation (D20) to the clad, $\dot{v}$ was taken to be zero. Also, it must be recognized that equation (B4), which was utilized in the derivation of equation (D20), is an empirical equation and does not specify the absolute sign of the strain rate. Therefore, the stress must be inserted as a positive value and the strain rate specified as positive or negative depending on whether the stress is positive (tensile) or negative (compressive).

Combining equations (D27) and (D28) to eliminate the pressure p_m at the interface yields

$$\frac{3\dot{\epsilon}_{tm}}{\dot{v}} = 1 - \frac{a_f}{a_c^{n_f/n_c}} \frac{\left(\frac{3\dot{\epsilon}_{tm}}{\dot{v}}\right)^{n_f/n_c}}{\left(\frac{\dot{v}}{3}\right)^{1-(n_f/n_c)}} \left[\left(\frac{\sqrt{3}}{2}\right)^{(1/n_f)-(1/n_c)} \left(\frac{\frac{-p_m}{B_c}}{\frac{p_m}{B_f}}\right) \frac{\left(1 + \frac{A_f}{\sqrt{3}}\right)^{1/n_f}}{\left(1 + \frac{A_c}{\sqrt{3}}\right)^{1/n_c}} \right]^{n_f} \tag{D29}$$

or

$$\alpha\left(\frac{3\dot{\epsilon}_{tm}}{\dot{v}}\right)^{n_f/n_c} + \frac{3\dot{\epsilon}_{tm}}{\dot{v}} - 1 = 0 \tag{D30}$$

where

$$\alpha \equiv \frac{a_f}{a_c^{n_f/n_c}} \left(\frac{3}{v}\right)^{1-(n_f/n_c)} \left(\frac{\beta_c}{\beta_f}\right)^{n_f} \tag{D31}$$

$$\beta_f = \left[\frac{2}{\sqrt{3}} \frac{\left(\frac{p_m}{B_f}\right)^{n_f}}{\left(1 + \frac{A_f}{\sqrt{3}}\right)} \right]^{1/n_f} \tag{D32a}$$

and

$$\beta_c = \left[\frac{2}{\sqrt{3}} \frac{\left(\frac{-p_m}{B_c}\right)^{n_c}}{\left(1 + \frac{A_c}{\sqrt{3}}\right)} \right]^{1/n_c} \tag{D32b}$$

The quantity β is a function only of n and the radius ratio φ_a or φ_b. The latter is evident from equations (D23) and (D25) or (D24) and (D26). Values of β were computed by numerical integration of equations (D25) and (D26) to determine A and by numerical

integration of equations (D23) and (D24) to determine p_m/B. The results of these computations for β and A are shown in figures 2 and 3.

The tangential strain rate at the fuel-clad interface can be obtained from equations (D30) and (D31), and figure 2. All other strain rates can be written in terms of the tangential strain rate at the interface.

Equation (D20a) may be rewritten as

$$\dot{\epsilon}_t = \frac{\dot{v}}{3} - \frac{\left(\frac{\dot{v}}{3} - \dot{\epsilon}_{tm}\right)\left(1 + \frac{A\varphi^2}{\sqrt{3}}\right)}{\varphi^2\left(1 + \frac{A}{\sqrt{3}}\right)} \tag{D33}$$

Equation (D20b) may be rewritten as

$$\dot{\epsilon}_r = \frac{\dot{v}}{3} + \frac{\left(\frac{\dot{v}}{3} - \dot{\epsilon}_{tm}\right)\left(1 - \frac{A\varphi^2}{\sqrt{3}}\right)}{\varphi^2\left(1 + \frac{A}{\sqrt{3}}\right)} \tag{D34}$$

Then from equation (D5)

$$\dot{\epsilon}_z = C_1 = \frac{\dot{v}}{3} + \frac{2A\left(\frac{\dot{v}}{3} - \dot{\epsilon}_{tm}\right)}{\sqrt{3}\left(1 + \frac{A}{\sqrt{3}}\right)} \tag{D35}$$

When applying equations (D33), (D34), and (D35) to the clad $\dot{v}$ is taken to be zero.

The strain rates are a function of time t and must be integrated with respect to time to obtain the strain in the time period from time zero to time t as follows

$$\epsilon = \int_0^t \dot{\epsilon}\, dt \tag{D36}$$

Equations for radial, tangential, and axial stress can be rewritten in terms of the constants evaluated from the boundary conditions. Solving for the radial stress at the

fuel-clad interface p_m from equation (D28) and substituting for B/p_m from equation (D32b)

$$\sigma_{rm} = -p_m = \left(\frac{\dot{\epsilon}_{tm}}{a_c}\right)^{1/n_c} \frac{2}{\sqrt{3}} \beta_c \tag{D37}$$

The tangential and axial stresses at the inner and outer surfaces of the fuel and clad cylinders relative to p_m are obtained from equations (D18) and (D19) using the definition of β (eqs. (D32a) and (D32b)):

$$\frac{\sigma_{tmf}}{p_m} = -1 - \frac{1}{\left(1 + A_f^2\right)^{(n_f-1)/2n_f}\left[\frac{\sqrt{3}}{2}\left(1 + \frac{A_f}{\sqrt{3}}\right)\right]^{1/n_f} \beta_f}$$

$$\frac{\sigma_{ta}}{p_m} = -\frac{1}{\left(1 + A_f^2\varphi_a^4\right)^{(n_f-1)/2n_f}\varphi_a^{2/n_f}\left[\frac{\sqrt{3}}{2}\left(1 + \frac{A_f}{\sqrt{3}}\right)\right]^{1/n_f} \beta_f}$$

$$\frac{\sigma_{tmc}}{p_m} = -1 + \frac{1}{\left(1 + A_c^2\right)^{(n_c-1)/2n_c}\left[\frac{\sqrt{3}}{2}\left(1 + \frac{A_c}{\sqrt{3}}\right)\right]^{1/n_c} \beta_c}$$

$$\frac{\sigma_{tb}}{p_m} = \frac{1}{\left(1 + A_c^2\varphi_b^4\right)^{(n_c-1)/2n_c}\varphi_b^{2/n_c}\left[\frac{\sqrt{3}}{2}\left(1 + \frac{A_c}{\sqrt{3}}\right)\right]^{1/n_c} \beta_c}$$

$$\frac{\sigma_{zmf}}{p_m} = -1 + \frac{\sqrt{3}\,A_f - 1}{2\left(1 + A_f^2\right)^{(n_f-1)/2n_f}\left[\frac{\sqrt{3}}{2}\left(1 + \frac{A_f}{\sqrt{3}}\right)\right]^{1/n_f} \beta_f}$$

$$\frac{\sigma_{za}}{p_m} = \frac{\sqrt{3}\, A_f \varphi_a^2 - 1}{2\left(1 + A_f^2 \varphi_a^4\right)^{(n_f-1)/2n_f} \varphi_a^{2/n_f} \left[\frac{\sqrt{3}}{2}\left(1 + \frac{A_f}{\sqrt{3}}\right)\right]^{1/n_f} \beta_f}$$

$$\frac{\sigma_{zmc}}{p_m} = -1 - \frac{\sqrt{3}\, A_c - 1}{2\left(1 + A_c^2\right)^{(n_c-1)/2n_c} \left[\frac{\sqrt{3}}{2}\left(1 + \frac{A_c}{\sqrt{3}}\right)\right]^{1/n_c} \beta_c}$$

$$\frac{\sigma_{zb}}{p_m} = - \frac{\sqrt{3}\, A_c \varphi_b^2 - 1}{2\left(1 + A_c^2 \varphi_b^4\right)^{(n_c-1)/2n_c} \varphi_b^{2/n_c} \left[\frac{\sqrt{3}}{2}\left(1 + \frac{A_c}{\sqrt{3}}\right)\right]^{1/n_c} \beta_c}$$

REFERENCES

1. Friedrich, C. M.; and Guilinger, W. H.: CYGRO-2: A FORTRAN IV Computer Program for Stress Analysis of the Growth of Cylindrical Fuel Elements with Fission Gas Bubbles. Rep. WAPD-TM-547, Bettis Atomic Power Lab., Nov. 1966.

2. Wyatt, L. M.: The Behaviour of Fissile Material Under Irradiation at Elevated Temperatures. Rep. AERE-M/R-1750, United Kingdom Atomic Energy Authority, Sept. 1955.

3. Foreman, A. J. E.: Calculations on the Rate of Swelling of Gas Bubbles in Uranium. Rep. AERE-T/M-134, Gt. Brit. Atomic Energy Research Establishment, Mar. 1956.

4. Barnes, R. S.: A Theory of Swelling and Gas Release for Reactor Materials. J. Nucl. Mat., vol. 11, no. 2, Feb.-Mar. 1964, pp. 135-148.

5. Finnie, Iain; and Heller, William R.: Creep of Engineering Materials. McGraw-Hill Book Co., Inc., 1959.

6. Nelson, R. S.: The Influence of Irradiation on the Nucleation of Gas Bubbles in Reactor Fuels. J. Nucl. Mat., vol. 25, no. 2, Feb. 1968, pp. 227-232.

7. Anon.: Progress on High-Temperature Fuels Technology During February Through April, 1969. BMI-1864, Batelle Memorial Institute, May 1969, pp. 48-60.

8. Howe, J. P.; and Weber, C. E.: Limitations on the Performance of Nuclear Fuels, Reactor Science and Technology, vol. 4, no. 1, Mar. 1954, pp. 163-184.

TABLE I. - SELECTED DATA AND RESULTS FOR NUMERICAL EXAMPLE

Time, t, hr	Ratio of time to total irradiation time to achieve fraction b, t/τ	Fractional fuel volume change caused by gaseous fission products, x_g	True bulk strain rate caused by solid and gaseous fission products, $\dot{v}$	Quantity defined by equation (D31), α	Relative tangential strain rate at fuel-clad interface, $3\dot{\epsilon}_{tm}/\dot{v}$	Tangential strain rate at fuel-clad interface, $\dot{\epsilon}_{tm}$	Tangential strain at fuel-clad interface, δ_{tm}	Tangential strain at inner radius of fuel cylinder, δ_{ta}	Tangential strain at outer radius of clad cylinder, δ_{tb}	Axial fuel strain, δ_{zf}	Axial clad strain, δ_{zc}
0	0	0	0.180×10^{-5}	0.628	0.626	0.376×10^{-6}	0	0	0	0	0
5 000	.25	.021	.761	.708	.599	1.52	.006	-.004	.004	.016	-.002
10 000	.50	.059	1.02	.727	.593	2.02	.015	-.010	.011	.041	-.006
15 000	.75	.114	1.28	.740	.589	2.50	.026	-.019	.020	.073	-.010
20 000	1.00	.188	1.55	.752	.585	3.01	.041	-.030	.030	.114	-.015

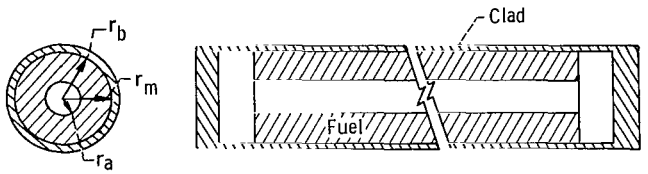

Figure 1. - Schematic drawing of cylindrical fuel element (fuel pin) showing fuel, clad, and void space.

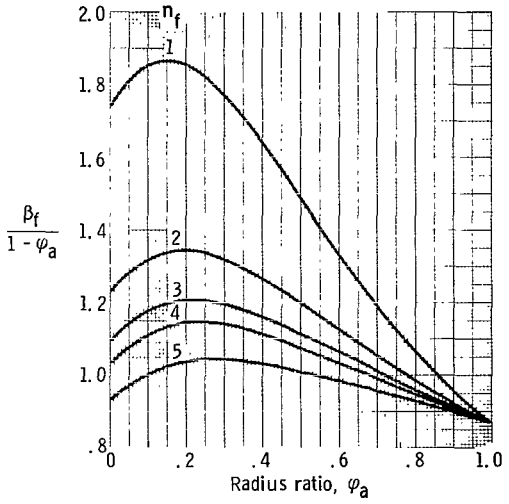

(a) Fuel cylinder.

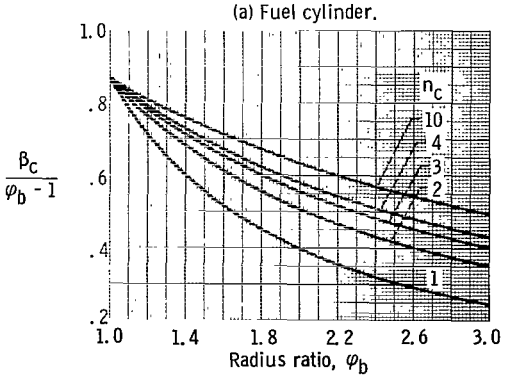

(b) Clad cylinder.

Figure 2. - The quantity β as function of radius ratio and n for fuel and clad cylinders, for use in equation (D31).

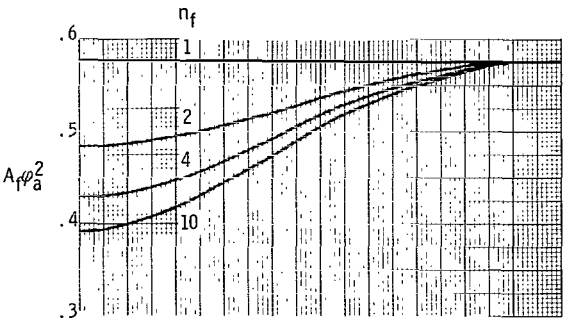

(a) Fuel cyclinder.

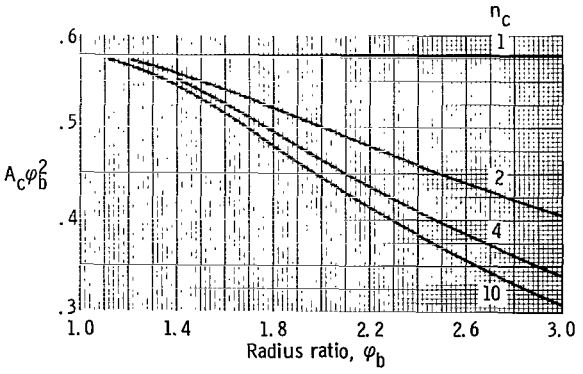

(b) Clad cylinder.

Figure 3. - The quantity A as function of radius ratio and n for use in equations (D33), (D34), and (D35).

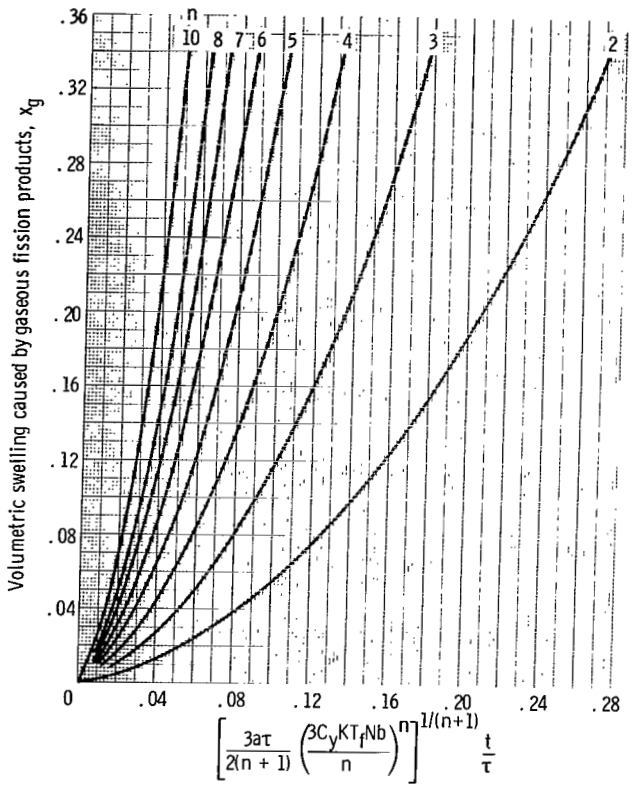

Figure 4. - Graphical presentation of equation (C23). Volumetric fuel swelling caused by gaseous fission products as function of parameter defining fuel characteristics, design conditions, and operating time.

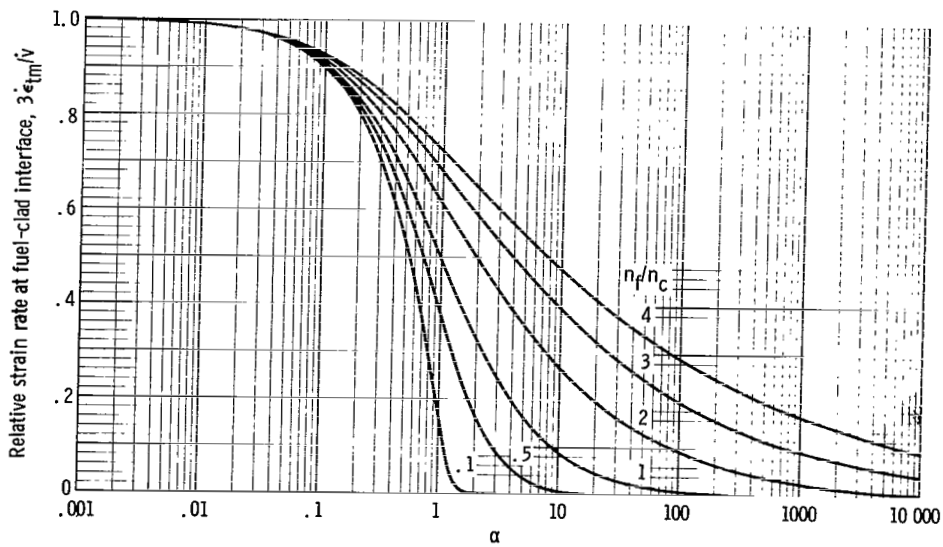

Figure 5. - Graphical presentation of equation (D30). Relative tangential strain rate at fuel-clad interface as function of parameter α defined by equation (D31).

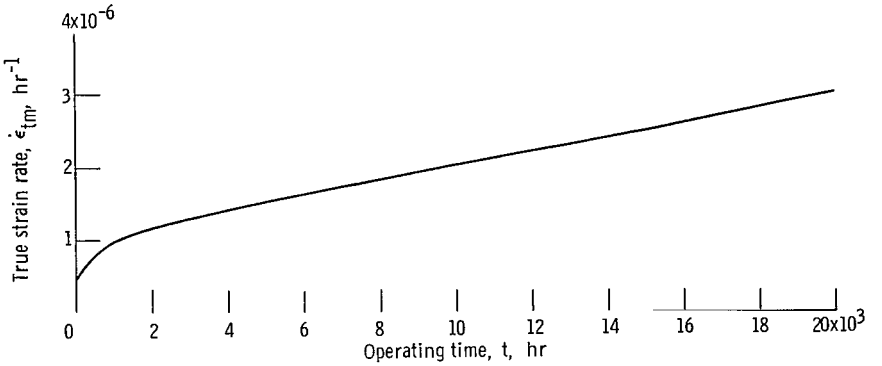

Figure 6. - True tangential strain rate at fuel-clad interface as function of operating time for numerical example.

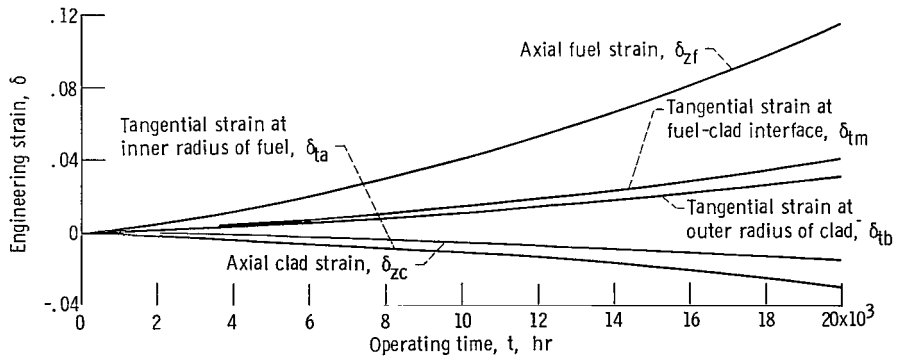

Figure 7. - Tangential and axial strains in fuel and clad as function of operating time for numerical example.

NATIONAL AERONAUTICS AND SPACE ADMINISTRATION
WASHINGTON, D. C. 20546

OFFICIAL BUSINESS

FIRST CLASS MAIL

POSTAGE AND FEES PAID
NATIONAL AERONAUTICS AND
SPACE ADMINISTRATION

"The aeronautical and space activities of the United States shall be conducted so as to contribute . . . to the expansion of human knowledge of phenomena in the atmosphere and space. The Administration shall provide for the widest practicable and appropriate dissemination of information concerning its activities and the results thereof."

—NATIONAL AERONAUTICS AND SPACE ACT OF 1958

NASA SCIENTIFIC AND TECHNICAL PUBLICATIONS

TECHNICAL REPORTS: Scientific and technical information considered important, complete, and a lasting contribution to existing knowledge.

TECHNICAL NOTES: Information less broad in scope but nevertheless of importance as a contribution to existing knowledge.

TECHNICAL MEMORANDUMS: Information receiving limited distribution because of preliminary data, security classification, or other reasons.

CONTRACTOR REPORTS: Scientific and technical information generated under a NASA contract or grant and considered an important contribution to existing knowledge.

TECHNICAL TRANSLATIONS: Information published in a foreign language considered to merit NASA distribution in English.

SPECIAL PUBLICATIONS: Information derived from or of value to NASA activities. Publications include conference proceedings, monographs, data compilations, handbooks, sourcebooks, and special bibliographies.

TECHNOLOGY UTILIZATION PUBLICATIONS: Information on technology used by NASA that may be of particular interest in commercial and other non-aerospace applications. Publications include Tech Briefs, Technology Utilization Reports and Notes, and Technology Surveys.

Details on the availability of these publications may be obtained from:

SCIENTIFIC AND TECHNICAL INFORMATION DIVISION

NATIONAL AERONAUTICS AND SPACE ADMINISTRATION

Washington, D.C. 20546